Bull. Mater. Sci., Vol. 37, No. 5, August 2014, pp. 1153–1157. © Indian Academy of Sciences.

Microstructural evolution and mechanical properties of hypereutectic Al–Si alloy processed by liquid die forging

F F WU*, S T LI, G A ZHANG and F JIANG

School of Materials Science and Engineering, Liaoning University of Technology, Jinzhou 121001, China

MS received 6 July 2013; revised 7 October 2013

Abstract. **The microstructural evolution and mechanical properties of a hypereutectic Al–Si alloy processed by liquid die forging were investigated. It is found that the grain size of the primary Si was significantly reduced by liquid die forging with increased pressure. The volume fraction of eutectic silicon was decreased with increased pressure. By liquid die forging with pressure up to 180 MPa, the average size of the primary Si was reduced to about 18 μm, which results in the remarkable increase in the fracture strength and hardness of the hypereutectic Al–Si alloy.**

Keywords. **Mechanical properties; hypereutectic Al–Si alloy; liquid die forging.**

1. Introduction

Hypereutectic Al–Si alloys possess attractive properties, such as low specific gravity, high strength at elevated temperature, excellent resistance and low coefficient of thermal expansion (Mohamed *et al* 2009; Hekmat-Ardakan and Ajersch 2010; Sha *et al* 2012). Therefore, they are attractive candidate materials for automotive, aerospace and electronics fields, especially, where the alloys substitute for cast iron, when the engineering advantages of light weight and wear resistance are considered (Hekmat-Ardakan *et al* 2010; Choi and Li 2012).

Usually, the microstructure of hypereutectic Al–Si alloys is composed of the primary Si crystals and the eutectic mixture of α-Al and eutectic Si. The size, morphology and distribution of the primary and eutectic Si play important roles in determining the mechanical properties and wear behaviours of the hypereutectic Al–Si alloys. However, by conventional casting processes, the primary Si crystals exist in the shape of star-like, polygonal, plate-like and feathery shape, and the eutectic Si is coarse and acicular, which is prone to premature crack initiation and fracture under tension and severely deteriorates the mechanical properties of hypereutectic Al–Si alloys (Yi and Zhang 2003). Generally, fine, spherical and uniformly distributed primary and eutectic Si crystals can improve the mechanical properties and tribological properties of hypereutectic Al–Si alloys (Liu *et al* 2011). Therefore, many efforts have been made to investigate the refinement and the morphological evolution of the primary and eutectic Si phases in Al–Si alloys such as adding modifiers (Dahle *et al* 2005), semi-solid processing (Jung *et al* 2001), superheating treatment of the melt (Chen *et al* 2005), electromagnetic field treatment (Lu *et al* 2007) and quench modification (Uzun *et al* 2004; Song *et al* 2007; Wang *et al* 2011). Chemical elements such as Sr, Na, Ce, Sc, La, Y, Yb and Er (McDonald *et al* 2004; Lu *et al* 2005; Prukkanona *et al* 2009; Tsai *et al* 2009; Nogita *et al* 2010; Xing *et al* 2010a; Li *et al* 2011a, b; Srirangam *et al* 2011; Vončina *et al* 2011) can effectively change the morphology of the eutectic Si from coarse needle- or flake-like to fine coral structure. Meanwhile, some studies proved that the primary Si of hypereutectic Al–Si alloys can be successfully refined by adding red phosphorus, phosphate salt, Al–P or Cu–P master alloys to form AlP particles as the nucleation agents for primary Si crystals (Wang *et al* 2009). Misch metals, such as Sc, Er and Ce can also significantly refine the primary Si in hypereutectic Al–Si alloys (Chang *et al* 1998; Zhang *et al* 2006; Xing *et al* 2010b; Kilicaslana *et al* 2012).

However, processed by adding modifier, the grain size of the primary Si crystals can only be reduced to be about 50 μm, which is not fine enough for enhancing the performance of hypereutectic Al–Si alloys. Therefore, it is still necessary to further refine the primary Si in hypereutectic Al–Si alloys by combining the modification and other processing techniques. Liquid die forging will be a potential candidate for these techniques. In liquid die forging, the high pressure (several hundred MPa) can cause a high coefficient of heat transfer and nonequilibrium solidification (Wu and Chin 1991; Murali and Yong 2010). It is a hybrid of conventional casting and forging technique, which combines economics and shape capability of castings with the strength and confidence level of forging

*Author for correspondence (ffwoo@foxmail.com)

(Murali and Yong 2010). Casting under forging pressure can results in pore free and fine microstructures with superior mechanical properties (Begg 1992). Therefore, liquid die forging should be an effective method for producing hypereutectic Al–Si alloys with fine microstructure and excellent mechanical properties. In the present work, liquid die forging is applied to treat a hypereutectic Al–Si alloy, and the microstructural evolution and mechanical properties are investigated.

2. Experimental

The selected hypereutectic Al–Si alloy has a nominal chemical composition of Si (18 wt%), Cu (4·5 wt%), Mn (0·1 wt%), Mg (0·65 wt%), Zn (0·1 wt%), Ti (0·2 wt%) and Al (balance). All pure metals or master alloys were melted in a resistance furnace. P–RE–Sr (RE is a Ce-rich rare-earth alloy) combined modifier was added to the melt to refine the primary and eutectic Si: first, 0·8% Al–3·5P was added at the temperature of 1098 K and the temperature was held for 20 min; second, 3% Al–10RE was added at 1098 K and the temperature was held for 10 min; third, the temperature was decreased to 1033 K and then 0·5% Al–10Sr was added and the temperature was held for 30 min; finally, the melt was finally held at 1093 K for casting. The liquid die forging was conducted in a commercial hydrostatic machine with specified load of 3 MN. The mould was made of 40Cr steel with hardness of HRC50. The puncher was made of 12CrMoV with hardness larger than HRC50. Before liquid die forging, the mould was held at 513 K and the melt was finally held at 1093 K for casting. The forging pressure was changed from 0 to 180 MPa. The pressurization rate is 10 MPa/s and the dwell time was 60 s. The microstructure was observed by a Zeiss optical microscope (OM) and a Hitach 3000S scanning electron microscope (SEM). The gauge dimension of the tensile sample was ∅ 8 mm × 45 mm (diameter × length). All mechanical tests were performed with a SANS CMT5305 testing machine at room temperature. The rate of the crosshead is 0·1 mm s^{-1}. A extensometer was used for measuring the strain. After tests, all the samples were observed by using SEM to reveal the deformation and fracture features.

3. Results and discussion

3.1 *Microstructure of hypereutectic Al–Si alloy processed by liquid die forging*

Figures 1 and 2 show the microstructure evolution of hypereutectic Al–Si alloy under different liquid-die-forging pressure, which demonstrates a substantial microstructural evolution in size and morphology of the primary Si crystals. When the pressure was 0 MPa, the average grain size of the primary Si was about 42 μm, and the distribution of the primary and eutectic Si was very non-uniform (figure 1a). When the pressure was increased up to 110 MPa, the average size of the primary Si was reduced to about 30 μm and the eutectic Si was also distributed more homogeneously (figure 1b). When the pressure was increased up to 140 and 180 MPa, the average size of the primary Si was decreased to be about 25 and 18 μm, respectively (figure 1(c and d)). Meanwhile, with the liquid die-forging pressure increasing, the eutectic Si was decreased gradually, as shown in figure 1.

Both the grain size and the volume fraction of the primary Si phase decrease in the hypereutectic Al–Si alloy solidification at liquid die forging, which can be attributed to the decrease in the diffusivity and the extended solid solution under high pressure. Meanwhile, high pressure will increase the melting point for Al and decrease the melting point for Si, which will change the phase diagram (Brazhkina *et al* 1991; Wu and Chin 1991; Yu *et al* 1999; Li *et al* 2012). It is measured that the melting point for Al increases to 6·4 K, when the pressure enhances 100 MPa. According to Clapeyron equation (Yu *et al* 1999)

$$\mathrm{d}T = \frac{T_\mathrm{m}(V_2 - V_1)}{\Delta H_\mathrm{m}}\mathrm{d}P, \tag{1}$$

where dP is the pressure change, dT the change of melting point with dP, T_m the melting point, V_1 the volume of 1 kg solid alloy, V_2 the volume of 1 kg liquid alloy and ΔH_m the melting latent heat. It can be calculated from (1) that the melting point for Al increases. But the melting point for Si decreases because the volume for Si contracts when it melts. Therefore, under high pressure, the eutectic point transfers to higher temperature and larger Si content, which decreases the volume fraction of the primary Si in the hypereutectic Al–Si alloy. Meanwhile, the liquid die-forging pressure can increase the supercooling of hypereutectic Al–Si melt, which leads to increase in nuclei for the primary Si and the refinement of the primary Si (Murali and Yong 2010). Meanwhile, the increased pressure can reduce the diffusion coefficient of the solute element Si in the melt, resulting in the homogeneous distribution of the alloying element Si in the melt, and increasing the supersaturation of the alloying element Si. Moreover, with the supercooling increasing, the solidification rate increased, which was beneficial to form the supersaturated solid solution (Yu *et al* 2000; Hong and Zeng 2002). As to the hypereutectic Al–Si alloy, with the pressure increasing, the alloy melt stayed in a supersaturated state, leading to the Al enrichment in front of the interface and reduction of the eutectic silicon. Therefore, with increasing pressure, both the primary and eutectic Si can be effectively refined.

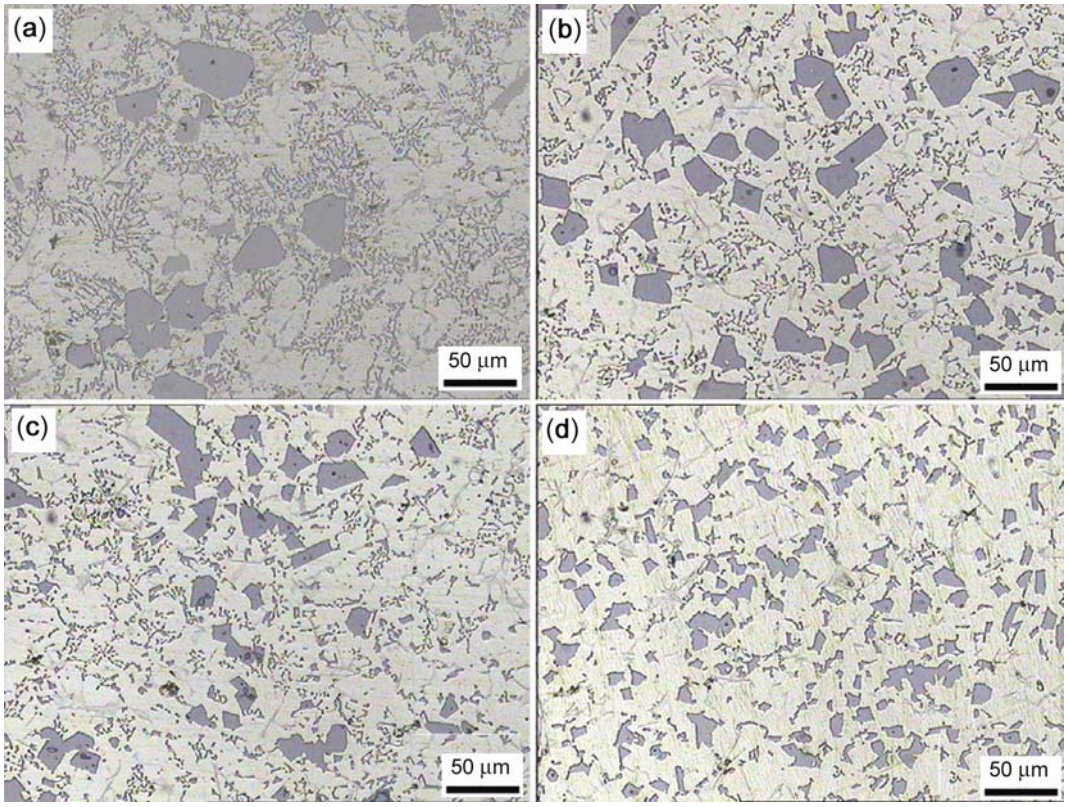

Figure 1. OM images showing the microstructural evolution of the hypereutectic Al–Si alloy processed under pressure of (**a**) 0, (**b**) 108·6, (**c**) 144·8 and (**d**) 181 MPa.

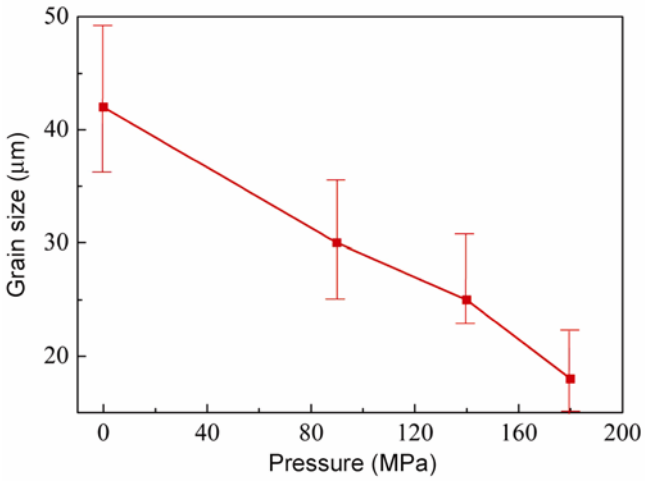

Figure 2. Evolution of grain size of the primary silicon for hypereutectic Al–Si alloy under different liquid-die-forging pressures.

3.2 *Mechanical properties of the hypereutectic Al–Si alloy processed by liquid die forging*

Figure 3(a) displays the fracture strength and elongation of the hypereutectic Al–Si alloys processed by liquid die forging. It is evident that the fracture strength was increased significantly with the pressure increasing, as shown in figure 3(a). When the pressure was 0 MPa, the fracture strength and elongation were 185 MPa and zero, respectively. However, when the pressure was increased to 180 MPa, the fracture strength was enhanced by 108·1% i.e. to 385 MPa, and the elongation was raised to 0·75%. Similarly, the correspondent hardness was increased from HRB78 to HRB84 with the pressure increased from 90 to 180 MPa. These results show that the liquid die-forging pressure is effective to enhance the mechanical properties of the hypereutectic Al–Si alloy.

The mechanical properties of the hypereutectic Al–Si alloy mainly depend on the size and morphology of the primary Si and eutectic Si crystals. In hypereutectic Al–Si alloys, the cracks easily initiate from the hard and brittle primary Si (Choi *et al* 2012; Kilicaslana *et al* 2012). The cracks may also come from the debonding of Si particles, and then propagate through the boundaries with α-Al phase (Chang *et al* 1998). The present results of tensile test show that the fracture strength and elongation of hypereutectic Al–Si alloy were significantly improved by liquid die forging. This is because that the refinement of primary Si and eutectic Si can decrease or eliminate premature cracks initiation and fracture under tension.

Figure 4 presents the fractographs of the hypereutectic Al–Si alloy processed by liquid die forging. For the sample without liquid die forging (i.e. pressure is 0 MPa), the fracture surface was mainly characterized with cleavage

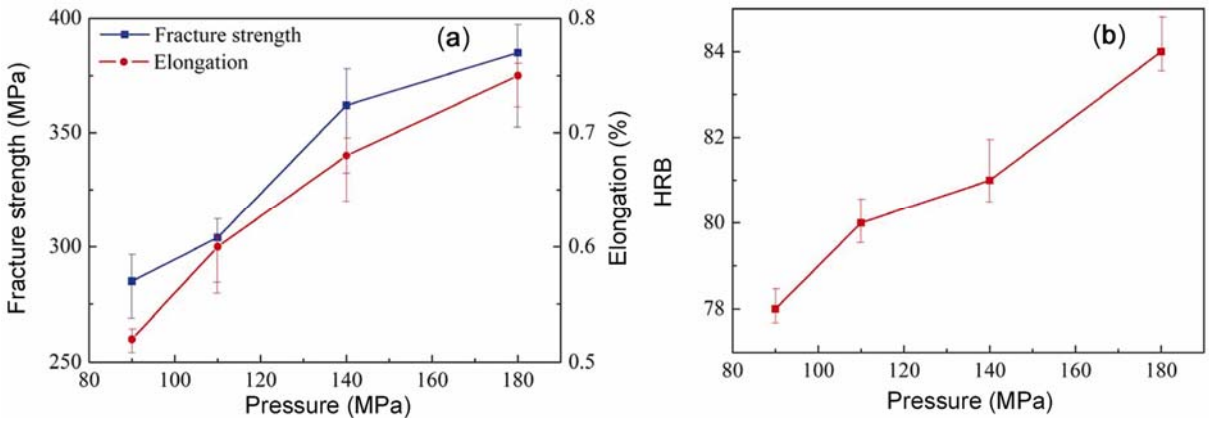

Figure 3. (**a**) Fracture strength and elongation and (**b**) Brinell hardness for liquid die-forged hypereutectic Al–Si alloy.

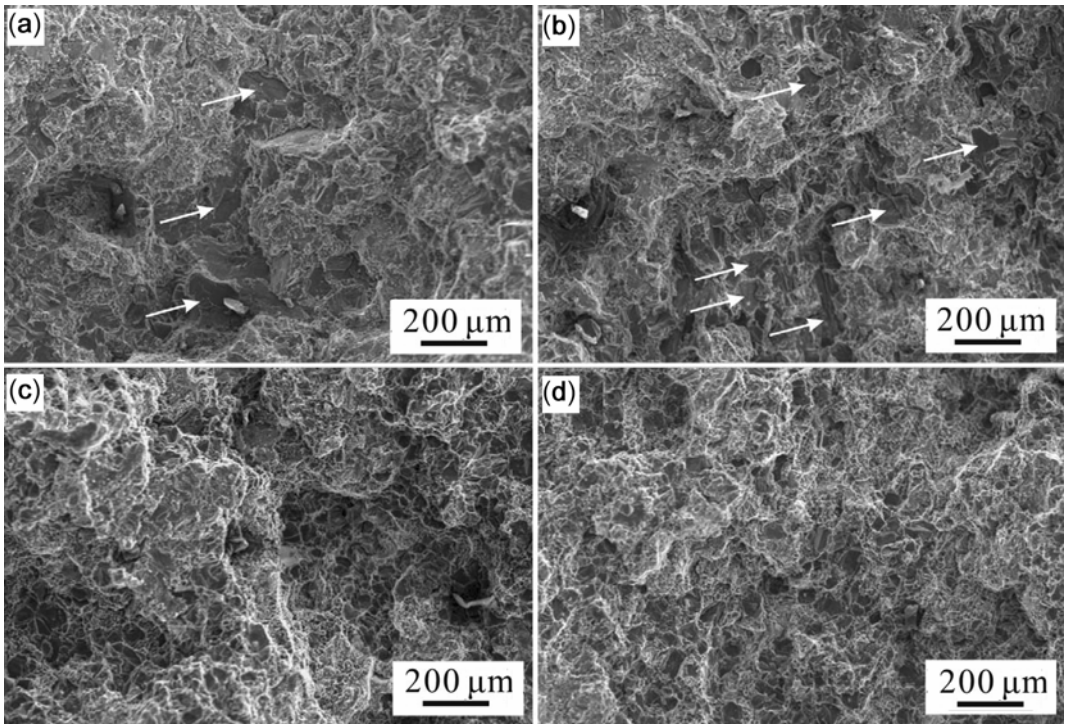

Figure 4. SEM images showing the tensile fracture features of the hypereutectic Al–Si alloy under different liquid die-forging pressures of (**a**) 90·5, (**b**) 108·6, (**c**) 144·8 and (**d**) 181 MPa.

planes and large crack sites in the primary Si phase, as shown in figure 4(a). When the pressure was increased up to 110 and 140 MPa, respectively, the fracture surfaces were covered by small crack planes in the refined primary Si phase and dimples in the eutectic matrix (figure 4(b and c)). Figure 4(d) shows the fractograph of the hypereutectic Al–Si alloy processed with the pressure of 180 MPa. It is clear that many dimples were formed on the fracture surfaces. These results indicate that a transition from a brittle failure for the sample without liquid die forging to a ductile failure for the sample with liquid die forging.

The fracture of hypereutectic Al–Si alloys was mainly attributed to three factors (Zhou and Duszczyk 1990): (a) the size and distribution of the primary and eutectic Si crystals, (b) the bonding strength between the Si crystals and the eutectic matrix, and (c) the crack of the Si crystals. The present fracture morphology shows an intragranular failure mainly caused by the coarse primary Si crystals, and there are more cracks in the coarse primary Si than the finer primary Si, as shown in figure 4. With the load increasing, the flow stress increase in the matrix and lead to a stress concentration near the primary Si crystals under tensile testing. The primary Si will fracture, when the local tensile stress exceeds the intrinsic fracture stress of the primary Si. In addition, cracks primarily initiate and propagate along the interfaces between primary Si crystals and Al matrix. When the neighbouring cracks

link with each other, the fracture of the hypereutectic Al–Si alloys finally occurs (Xu *et al* 2007). In this work, the liquid die-forging pressure significantly decreased the size and changed the morphology of primary Si and eutectic Si crystals. Based on fracture mechanics (Mayers and Chawla 1999), the relation between the intrinsic fracture stress σ_F on the primary Si and the length L of the internal defects can be expressed by

$$\sigma_F = \left(\frac{2E\gamma}{\pi L}\right)^{1/2}. \quad (2)$$

Here γ and E are the fracture surface energy and the Young's modulus of the particles, respectively. According to (2), the internal defects of coarse primary Si crystals are much longer than fine Si crystals, which results in lowering the intrinsic fracture stress. Therefore, the refinement of the primary Si crystals can effectively enhance the tensile strength and the elongation of hypereutectic Al–Si alloy by liquid die forging.

4. Conclusions

In summary, the grain size of the primary Si in a hypereutectic Al–Si alloy was remarkably reduced by liquid die forging. By liquid die forging with pressure up to 180 MPa, the average size of the primary Si was reduced to be about 18 μm. The volume fraction of the eutectic silicon was also decreased with the increased pressure. The refinement of the microstructure significantly enhances the fracture strength and hardness of the hypereutectic Al–Si alloy.

Acknowledgements

This work was financially supported by the Education Department of Liaoning Province of China under Grant Nos 2009S053 and LT2010051.

References

Begg J 1992 *Process optimization in the squeeze casting of zinc–aluminum alloys and composites* (UK: Loughborough University of Technology)

Brazhkina V V, Popov S V, Voloshina R N, Stanev L M and Spirov I G 1991 *High Press. Res.* **6** 333

Chang J Y, Moon I and Choi C S 1998 *J. Mater. Sci.* **33** 5015

Chen Z W, Jie W Q and Zhang R J 2005 *Mater. Lett.* **599** 2183

Choi H S, Konishi H and Li X C 2012 *Mater. Sci. Eng.* **A541** 159

Choi H S and Li X C 2012 *J. Mater. Sci.* **47** 3096

Dahle A K, Nogita K, McDonald S D, Dinnis C and Lu L 2005 *Mater. Sci. Eng.* **A413–414** 243

Hekmat-Ardakan A and Ajersch F 2010 *Acta Mater.* **58** 3422

Hekmat-Ardakan A, Liu X C, Ajersch F and Chen X G 2010 *Wear* **269** 684

Hong S Z and Zeng Z P 2002 *Spec. Cast. Nonferr. Alloys* **22** 26

Jung H K, Seo P K and Kang C G 2001 *J. Mater. Process. Technol.* **113** 568

Kilicaslana M F, Lee W R, Lee T H, Sohn Y H and Hong S J 2012 *Mater. Lett.* **71** 164

Li B, Wang H W, Jie J C and Wei Z J 2011a *Mater. Des.* **32** 1617

Li B, Wang H W, Jie J C and Wei Z J 2011b *J. Alloys Compd.* **509** 3387

Li L X, Zong H T, Li M, Wang H X and Cai H X 2012 *High Temp.-High Pres.* **41** 69

Liu G, Li G D, Cai A H and Chen Z K 2011 *Mater. Des.* **32** 121

Lu D H, Jiang Y H, Guan G S, Zhou R F, Li Z H and Zhou R 2007 *J. Mater. Process. Technol.* **189** 13

Lu L, Nogita K and Dahle A K 2005 *Mater. Sci. Eng.* **A399** 244

Mayers M A and Chawla K K 1999 *Mechanical behaviour of materials* (Upper Saddle River, New Jersey: Prentice Hall)

McDonald S D, Nogita K and Dahle A K 2004 *Acta Mater.* **52** 4273

Mohamed A M A, Samuel A M, Samuel F H and Doty H W 2009 *Mater. Des.* **30** 3943

Murali S and Yong M S 2010 *J. Mater. Process. Technol.* **210** 1276

Nogita K, Yasuda H, Yoshida M, McDonald S D, Uesugi K, Takeuchi A and Suzuki Y 2010 *J. Alloys Compd.* **489** 415

Prukkanona W, Srisukhumbowornchai N and Limmaneevichitr C 2009 *J. Alloys Compd.* **477** 454

Sha M, Wu S S, Wang X T, Wan L and Ping A 2012 *Mater. Sci. Eng.* **A535** 258

Song K K, Bian X F, Guo J, Wang S H, Sun B A, Li X L and Wang C D 2007 *J. Alloys Compd.* **440** L8

Srirangam P, Kramer M J and Shankar S 2011 *Acta Mater.* **59** 503

Tsai Y C, Chou C Y, Lee S L, Lin C K, Lin J C and Lim S W 2009 *J. Alloys Compd.* **487** 157

Uzun O, Karaaslan T, Gogebakan M and Keskin M 2004 *J. Alloys Compd.* **376** 149

Vončina M, Kores S, Mrvar P and Medved J 2011 *J. Alloys Compd.* **509** 7349

Wang E D, Hui X D, Wang S S, Zhao Y F and Chen G L 2011 *Mater. Sci. Eng.* **A528** 5764

Wang Y P, Wang S J, Li H and Liu X F 2009 *J. Alloys Compd.* **477** 139

Wu H and Chin B A 1991 *J. Mater. Sci.* **26** 993

Xing P F, Gao B, Zhuang Y X, Liu K H and Tu G F 2010a *J. Rare Earths* **28** 927

Xing P F, Gao B, Zhuang Y X, Liu K H and Tu G F 2010b *Acta Metall. Sin.* **23** 327

Xu C L, Wang H Y, Yang Y F and Jiang Q C 2007 *Mater. Sci. Eng.* **A452–453** 341

Yi H K and Zhang D 2003 *Mater. Lett.* **57** 2523

Yu X F, Zhang G Z, Wang X Y, Gao Y Y, Jia G L and Hao Z Y 1999 *J. Mater. Sci.* **34** 4149

Yu X F, Zhang G Z, Xiao H J, Pan A S, Jia G L, Gao Y Y, Hao Z Y and Guo X B 2000 *Chin. J. Mater. Res.* **14** 141

Zhang H H, Duan H L, Shao G J, Xu L P, Yin J L and Yan B 2006 *Rare Metals* **25** 11

Zhou J and Duszczyk J 1990 *J. Mater. Sci.* **25** 4541